Stochastic Dynamics Modeling and Motion Control of Optically Trapped Microspheres

Keshav Rajasekaran

A thesis submitted in fulfillment
of the requirements for the degree of

Master of Science in Mechanical Engineering

University of Washington

2017

Committee:

Ashis Banerjee, Chair

Sam Burden

Sawyer Fuller

Program Authorized to Offer Degree:
Department of Mechanical Engineering

University of Washington

Abstract

Stochastic Dynamics Modeling and Motion Control of Optically Trapped Microspheres

Keshav Rajasekaran

Chair of the Supervisory Committee:
Professor Ashis Banerjee
Department of Mechanical Engineering and Industrial and Systems Engineering

This master's thesis describes the dynamics of micro-spheres in a Optical Tweezers environment and details the design of a controller to manipulate optically trapped micro-spheres.

- It expounds on the highly stochastic dynamics of the micro-spheres in a fluid medium and details the effect of all relevant forces with respect to the Optical Tweezers.

- It dwells into details around the construction of a Model Predictive Controller to manipulate optically trapped micro-spheres.

TABLE OF CONTENTS

LIST OF FIGURES

ACKNOWLEDGMENTS

This theis has in no way been a solo effort and I would like to thank everybody I hold accountable for its successful completion. My advisor Asst Prof Ashis Banerjee for the endless patience, guidance, valuable feedback and funding during the course of the thesis. The faculty who's classes have helped me grasp the fundamental concepts in control and planning. Wanwisa Kisalang and Kate Gayle who have helped through all the forms and office work throughout my stay here at the University of Washington.

Also, I would like to thank my parents without whom I would not have been able to pursue my masters.

A special thanks to John Stewart for helping with the experimentation and for the company when the experiments did not go as planned.

DEDICATION

To those who say playing with lasers will get you nowhere.

Chapter 1
INTRODUCTION

Be it being able to draw water from an aquifer using a pulley or utilizing levers to gain a mechanical advantage, manipulation and control of objects are the objectives around which humanity achieved its growth as a scientific society. After all these years we are still obsessed with the same objectives of being able to control and manipulate objects accurately but at a scale so small that the objects can't be seen by the naked eye. This section will cover the uses and need for micro-manipulation and the various techniques that are present for the same today.

1.1 Micro-manipulation

With the advances in imaging techniques we now have a way to view objects in the order of microns from biological cells to the building blocks of a crystal. To be able to study their interactions, forces and test the properties at this scale a precise and accurate means of manipulation at this scale is a necessity. Various techniques have been developed to achieve this leveraging a range of physical mechanisms. Some of the more widely used ones are microfluidics, magnetic tweezers, and optical tweezers. These are used extensively in biological studies though they do find use in material design and micro structure assemblies.

1.1.1 Microfluidics

Microfluidics comprises of a set of techniques that deals with the precise control of a small volume of fluid. Though it started as a means to develop inkjet print heads recently the techniques have been adapted to help with cell studies [1, 10]. It is used frequently in cell sorting experiments to separate cells of interest from a homogeneous mixture[11]. These

techniques are limited by an external apparatus that constraints fluid flow to achieve the necessary separation. Further the object in question is not directly in control rather it is the flow of the fluid that is controlled and differences in some other physical property is relied upon to achieve the necessary separation.

1.1.2 Magnetic Tweezers

Magnetic tweezers work by initially trapping a object in a magnetic potential well and then using the trapped object to manipulate the object of interest. The trapped object can be controlled by varying the strength of the magnetic field. It is used widely in cell stiffness measurement and general micro manipulation. The advantage of using magnetic tweezers is that it does not apply any forces directly to the cells or objects being manipulated this prevents damage during manipulation of sensitive cells and materials. But the system still has a few shortcomings, direct manipulation of the object is limited to magnetic materials only. Further individual multiplexing is not trivially achieved by the magnetic tweezers setup and even then is not scalable.

1.1.3 Optical Tweezers

Optical tweezers create a potential well due to the refraction of light. The mechanics of the trapping mechanism will be explained in detail over the next few sections. Optical tweezers can be used in conjunction with other methods described or as a stand alone system for cell-sorting or aggregation experiments. The system requires more care to handle sensitive material but they can be multiplexed easily and if leveraged can greatly increase the utility of the system.

With the increasing interest in study biological and structural systems at the molecular level there is an increasing need for high throughput micro-manipulation systems and the optical tweezers provides us with an opportunity to utilize its inherent multiplex-abilty for us to achieve this.

Chapter 2

OPTICAL TWEEZERS

Optical tweezers are tools that utilize a focused beam of light to hold and manipulate microscopic particles due to a difference in the refractive indexes of the medium and the object of interest.

2.1 Trapping Mechanism

The trapping mechanism can be explained by a multitude of theoretical approaches. The figure 2.1 explains the optical trapping mechanism using ray optics, which is the easiest way to understand it.The rays incident on the object is mostly refracted through it. As the ray refracts it undergoes a change in velocity and direction, a change in momentum. Newtons third law states there is a equal and opposite reaction to every action, so the change in momentum effects a reaction force on the object as shown by forces F_1 and F_2. Due to the Gaussian intensity profile of the beam F_1 is greater than F_2 thus causing a restorative force that keeps the object in the center of the beam. The total force is calculated by integrating over all rays in the beam. The object being trapped must have a higher refractive index than the medium it is present in. This a condition that must be satisfied for the trapping mechanism to work.

2.2 Holographic Optical Tweezers

The optical tweezers system that is most widely used nowadays is the Holographic Optical Tweezers(HOT). A schematic diagram of a HOT system is shown in Fig2.2 The key component of a HOT is the Spatial Light Modulator(SLM). The SLM acts as a variable diffraction gradient and by projecting a computer generated hologram onto to the SLM the

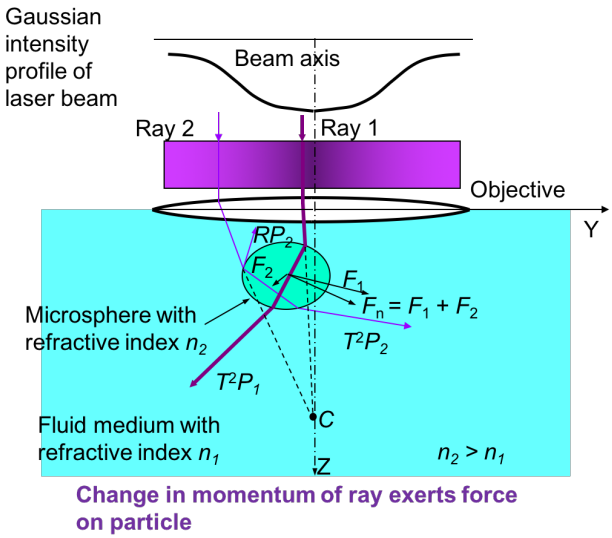

Figure 2.1: Principle of Optical Trapping

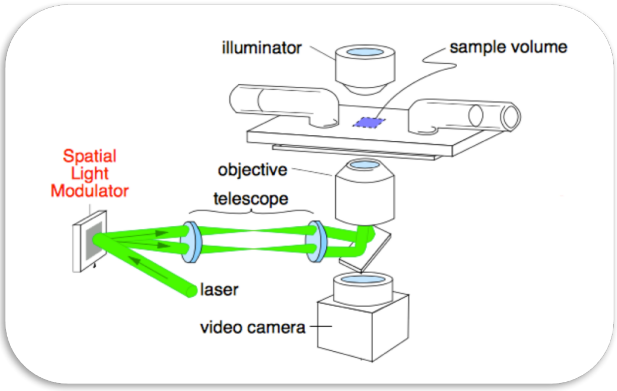

Figure 2.2: Holographic Optical Tweezers Setup

Source: [27]

HOT achieves three important functions.

1. It enables the HOT system to be multiplexed easily by projecting a diffraction pattern that achieves all optical traps required
2. Each of these multiplexed traps can be controlled individually in three dimensions
3. The light field itself can be manipulated

These functions provide the HOT system to be an ideal solution to the needs of research studies that require a large scale micro manipulation system. This thesis will detail a method to achieve such scalability so as to leverage these functionalities of the HOT system to the maximum. In the next section I will briefly discuss the literature of work done until now involving the optical tweezers, its control and the origins of the idea that I have re-purposed to achieve my goals.

Chapter 3

LITERATURE REVIEW

Since their inception by Ashkin in 1970[2], they have been used widely as they offer certain advantages over other forms of micro-scale manipulators such as micro-fluidic chambers and magnetic micro manipulators. They can be easily multiplexed through a programmable spatial light modulator, thereby providing us the ability to simultaneously and independently control multiple objects. They exert forces of the order of picoNewtons, and, hence, can be used to handle fragile and irregular-shaped objects like biological cells easily [65]. They are being increasingly used for various biophysical experiments such as cell sorting [62] and characterizing the mechanochemical properties of cells [38].

Owing to the small size scale and fast, stochastic dynamics of the problem, a vision based feedback system is a must to achieve any form of controllability of the manipulated objects. Though a human-in-the-loop controller is possible to use the multiplexing capabilities of the optical tweezers system, it does not easily lend itself to an automated setting. Automation not only improves the accuracy, precision, and repeatability of the system, but also provides us with the ability to surpass the human limitation of handling a larger number of objects simultaneously.

Substantial recent progress has been reported in the context of automated optical tweezers operations [7]. For example, photosensitive objects such as cells have been manipulated indirectly using optically-trapped beads [24, 26, 59, 5]. The complexities of the controllers to realize such manipulation vary from simple proportional derivative controllers [17] to controllers that employ stochastic programming and Markov chains [9, 64]. Observer based controllers have also been used to achieve automation [18]. Methods such as dynamic region control [46] and a combination of optical tweezers and microfluidic chambers[25] have been

studied to achieve viable automation of optical tweezers. Region based flocking algorithms have been studied to produce coordinated motion of a group of beads [19]. Various swarm inspired algorithms have also been developed to control multiplexed tweezers [23].

The other important aspect of automation is to be able to generate collision-free paths for the manipulated objects in a computationally efficient manner. Various robotic path planning techniques have been developed for this purpose. As an example, a rapidly-exploring random tree (RRT) has been used for cell transportation [39]. However, the number of objects that can be concurrently handled by these techniques are small, typically limited to only a few [60, 16].

Handling complex dynamic models, nonlinearities and uncertainties in control have been studied and mastered in the macroscopic world. Model Predictive Controllers(MPCs) have been utilized by the oil industry for a long time to control the fractional distillation process [28]. MPCs are able to utilize complex dynamic models to make current decisions based on future outcomes of the decision [53]. A lot of work as been done to adapt the MPC algorithm to handle nonlinearities [32]. MPC formulations have also been devised to handle uncertainties and disturbances that are inherent in any physical process [54, 52, 56]. Research has also been done on how best to computational efficiency of a MPC and understand the the stability, optimality of the solution [15, 49].

Similarly obstacle avoidance has also been achieved by roboticists using various methodologies [45, 41, 29, 37]. These algorithms have also been tested successfully on actual robot implementations in both known and unknown terrain and with a multiple robots[30, 66]. Work has also been done to improve the efficiency and the robustness of these algorithms so they can handle both uncertainties in the environment and in the robots own actuators and sensors [44, 43].

These two fields of study set up a good framework around which a real time controller that can handle the complexity while leveraging the multiplexabilty can be designed for the HOT system. This thesis dwells into how we can adapt these techniques that have been used reliably in the macro scale to the microscopic scale of the HOT system.

Chapter 4

TECHNICAL APPROACH

4.1 Dynamics Modeling

Before a MPC can be formulated a high accuracy dynamics model is necessary to describe the system we are trying to control. Though there are efficient ways to compute the forces for the HOT system they are computationally too expensive to be used along with a real time controller. Further these models are limited to forces between one optical trap or beam and one object. An accurate dynamic model of the effect of all resulting forces from all beam object interactions is essential to develop a controller that can achieve the desired levels of multiplexed action while being able to handle the inherent uncertainties that occur at the microscopic levels.

The key issues with describing the dynamics of microscopic objects in an optical trapping scenario are the effect of multiple traps and the inherent stochastic Langevin forces that arise due to the scale under consideration. Forces like the viscous drag and buoyancy also affect the dynamics of the system.

The optical trapping forces for a 2μm silica sphere is shown in Figure 4.1. The force can be clearly split into a linear zone and a non linear zone. So the trapping force is modeled as a spring with a linear stiffness term and a non-linear stiffness term. The equations for a system of p beams and n spheres in the work space are described next.

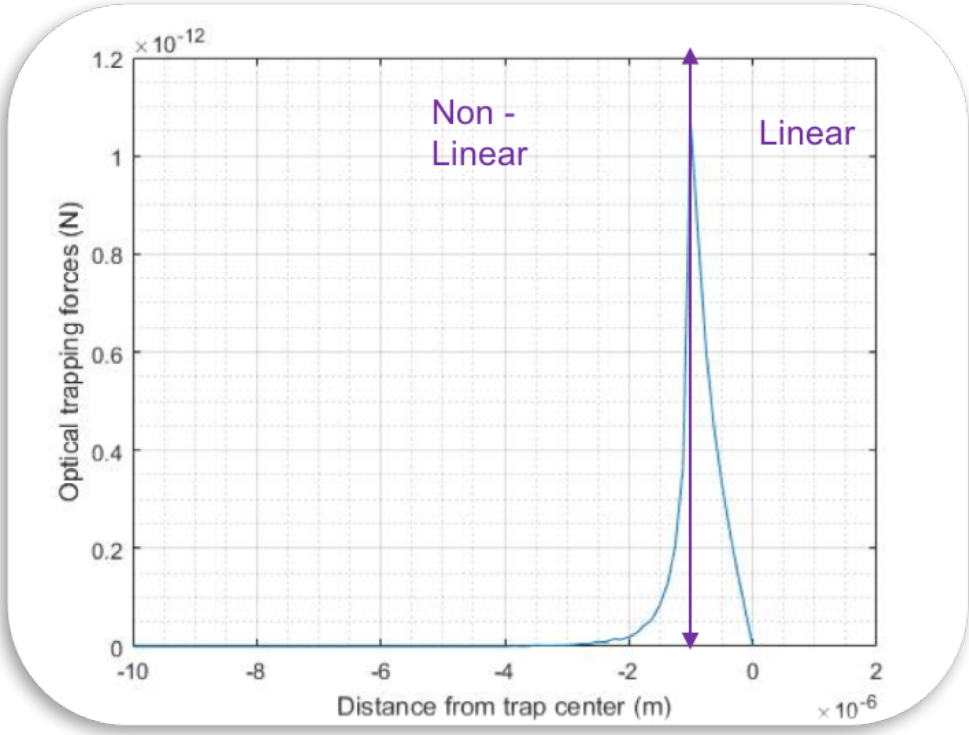

Figure 4.1: Principle of Optical Trapping

4.1.1 Equations

$$m_1\ddot{\mathbf{x}}_1(t) = (\mathbf{K}_{l1}(t)\circ(\mathbf{U(t)}-\mathbf{x}_1(t)\otimes\mathbf{1}^T)\circ-\mathbf{K}_{e1}\circ|(\mathbf{U}(t)-\mathbf{x_1}(t)*\mathbf{1}^T)|.^{-b})\mathbf{1}-\mathbf{B}_1\dot{\mathbf{x}}_\mathbf{1}(t)-\mathbf{B}_{o1}+\mathbf{F}\eta_\mathbf{1}.$$

$$\mathbf{y}_1 = \mathbf{C}\mathbf{x}_1 + \xi_\mathbf{1}. \tag{4.1}$$

$$m_2\ddot{\mathbf{x}}_2(t) = (\mathbf{K}_{l2}(t)\circ(\mathbf{U(t)}-\mathbf{x}_2(t)\otimes\mathbf{1}^T)\circ-\mathbf{K}_{e2}\circ|(\mathbf{U}(t)-\mathbf{x_2}(t)\otimes\mathbf{1}^T)|.^{-b})\mathbf{1}-\mathbf{B}_2\dot{\mathbf{x}}_2(t)-\mathbf{B}_{o2}+\mathbf{F}\eta_\mathbf{2}.$$

$$\mathbf{y}_2 = \mathbf{C}\mathbf{x}_2 + \xi_\mathbf{2}. \tag{4.2}$$

$$m_n\ddot{\mathbf{x}}_n(t) = (\mathbf{K}_{ln}(t)\circ(\mathbf{U(t)}-\mathbf{x}_n(t)\times\mathbf{1}^T)\circ-\mathbf{K}_{en}\circ|(\mathbf{U}(t)-\mathbf{x_n}(t)\times\mathbf{1}^T)|.^{-b})\mathbf{1}-\mathbf{B}_2\dot{\mathbf{x}}_\mathbf{1}(t)-\mathbf{B}_{on}+\mathbf{F}_n\eta_\mathbf{n}.$$

$$\mathbf{y}_n = \mathbf{C}\mathbf{x}_n + \xi_\mathbf{n}. \tag{4.3}$$

The set of equations model the dynamics of each sphere when subjected to multiple optical traps in its vicinity. Combining the equations provides us with an equation that governs the dynamics of all the n spheres.

$$M\ddot{\mathbf{x}}(t) = (\mathbf{K}_{ln}(t) \circ (\mathbf{1} \otimes \mathbf{U(t)} - \mathbf{x} \times \mathbf{1}^T) \circ a * e^{-\mathbf{K}_{en} \circ (1 \otimes \mathbf{U}(t) - \mathbf{x}(t) \times \mathbf{1}^T).^2})\mathbf{1} - \mathbf{B}_{drag}\dot{\mathbf{x}}(t) - \mathbf{B}_o + \mathbf{F}\eta$$

$$\mathbf{y} = \mathbf{C}\mathbf{x} + \xi. \tag{4.4}$$

Equation 4.4 provides us with a single governing equation for the dynamics of all beads in the work space. The definitions for the terms used are listed below:

- M is the $n \times n$ diagonal matrix populated by the mass of the respective sphere.
- $\mathbf{x}$, is a $3n\times$ 1 combined vector of the co-ordinates of the center of spheres.
- $\mathbf{K}_{ln}(t)$is a $3n \times p$ matrix for linear stiffness
  For all rows excpet every third row

  $$[l,k] \text{ entry of } \mathbf{K}_{ln}(t) = \begin{cases} k_r & [l,k] \text{ element of } \mathbf{U}(t) - \mathbf{x}_i \otimes \mathbf{1}^T < \delta \end{cases}$$

  For every third row

  $$[l,k] \text{ entry of } \mathbf{K}_{ln}(\text{t}) = \begin{cases} k_{a1} & [l,k] \text{ element of } \mathbf{U}(t) - \mathbf{x}_i \otimes \mathbf{1}^T < -\delta \ \&\& < 0 \\ k_{a2} & [l,k] \text{ element of } \mathbf{U}(t) - \mathbf{x}_i \otimes \mathbf{1}^T < \delta \ \&\& > 0 \end{cases}$$

- $\mathbf{K}_{ei}(t)$is a $3n \times p$ matrix for nonlinear stiffness

  $$[l,k] \text{ entry of } \mathbf{K}_{ei} = \begin{cases} 1 & \text{[l,k] element of } |\mathbf{U}(t) - \mathbf{x}_i \mid < \delta \\ k_2 & \text{depends on the displacement} \end{cases}$$

- k_r is the radial stiffness and is equal for x and y directions
- k_a is the axial stiffness and depends on the sign of z.

- k_2 is a curve fitting parameter for the nonlinear stiffness
- δ is the distance at which linearity is lost
- ϵ is the distance at which the trap has no effect on the sphere
- $\mathbf{U}(\mathrm{t})$ is a $3 \times p$ matrix of the co-ordinates of the focus of the laser traps
- $\mathbf{1}$ is a vector of ones of dimensions $p \times 1$
- $\circ$ denotes an element wise multiplication
- $\otimes$ denotes the Tensor Product or Kronecker Product
- e^A here describes a element wise exponent and not a matrix exponent
- $\mathbf{B}_{drag}$ is the viscous drag coefficient matrix of dimension $3n$ x $3n$ populated by $\begin{cases} 6\pi r\mu & \text{if it is not close to the cover slide} \\ \frac{6\pi r\mu}{1-\frac{9r}{16h}+\frac{r^3}{8h^3}-\frac{45r^4}{256h^4}-\frac{r^5}{16h^5}} & \text{if it is near the cover slide} \end{cases}$ μ is the viscosity of the medium and h is the distance between the cover-slip and center of the sphere
- $\mathbf{B}_o$ is the buoyant force it is a $3n \times 3n$ diagonal matrix with $\begin{cases} V\rho_l g & \text{every third diagonal element} \\ 0 & \text{othervise} \end{cases}$
- $\mathbf{F}$ is a diagonal disturbance coupling matrix with dimension 3x3 where each term is $\sqrt{\frac{2k_bT\gamma}{\delta t}}$ where k_b is the Boltzmann constant and γ is the drag coefficient. $\sqrt{2k_bT\gamma}$ is obtained via the fluctuation- dissipation theorem [63].
- $\mathbf{C}$ is the observation matrix
- η_i, ξ_i are white noise with variances equal to the differences in time between two samples

- $i \in \{1, \ldots, n\}$
- $\cdot^2$ is an elementary operation and not a matrix operation

4.1.2 Verification

To verify the dynamics equations, we developed a simulator using the Optical Tweezers in Geometrical Optics toolbox(OTGO)[14]. We used the simulations to verify the dynamic equations for multiple scenarios involving multiple traps and multiple beads. The simulations have provided results that correspond well to known theoretical solutions.

Equilibrium point

The first metric that we will discuss is the equilibrium point of the optical trap. This simulation verifies that all objects that are trapped by a beam are trapped at their theoretical equilibrium point irrespective of where they start. Figure 4.2 is the result of the simulation of two beads with one beam. As seen from the progression of images from left to right, the beam is successfully able to trap both beads. Irrespective of the starting point it is seen that the dynamics model correctly evaluates the final equilibrium position accurately.

Mean Squared Displacement

The second metric we will discuss is the simulation of the Brownian motion directly. To verify the formulation of the stochastic component of the dynamics equation is accurate we check that the final displacement experienced by the object under free diffusion is equal to the theoretical mean squared displacement for a freely diffusing particle. The theoretical mean squared displacement is given by

$$4Dt \tag{4.5}$$

where

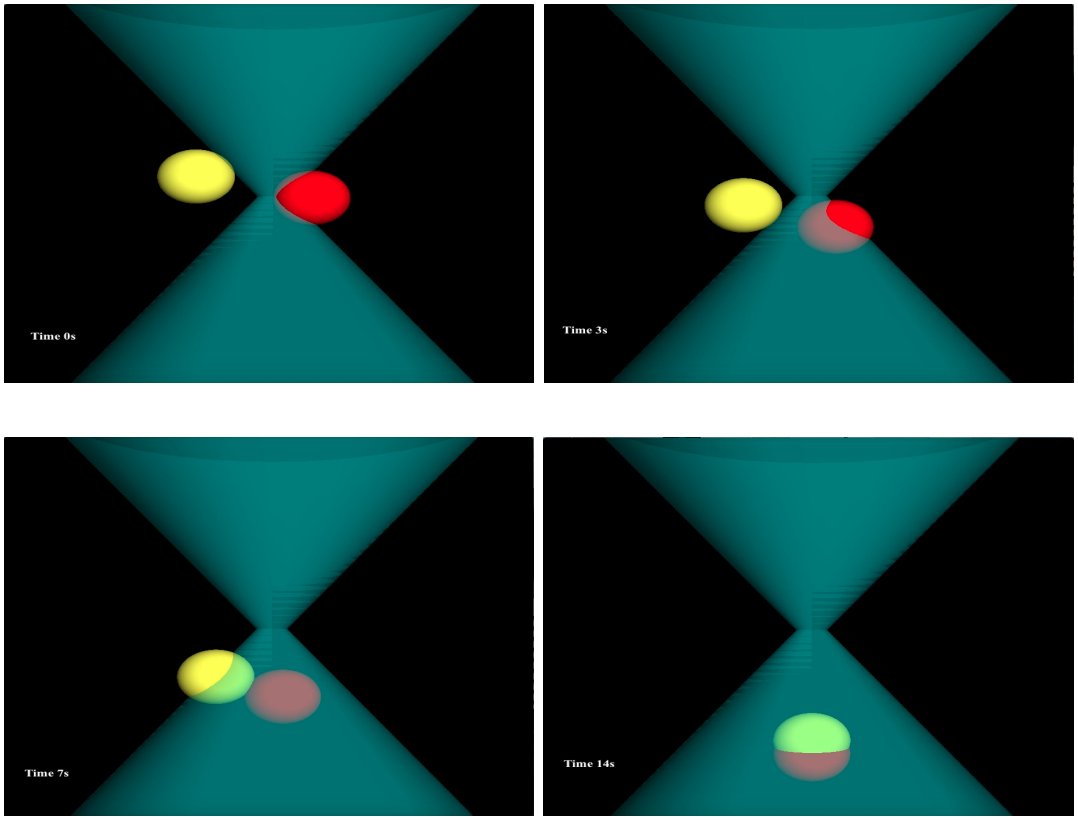

Figure 4.2: Simulation results of two beads influenced by one optical trap. The red bead starts at r=2.5μm and $\theta = 0^o$ and z=0. The yellow bead starts at r=5μm and $\theta = 45^o$ and z=-2.5μm. Both beads are of radius 5μm. The green area denotes the optical trap.

- D is the diffusion constant that can be calculated by using the Stokes-Einstein equation. So $D = \frac{k_B T}{6pi\eta r}$ where η is the viscosity and r is the radius of the object
- t is the total time that the diffusion is occurring for

As the data in Table 4.1 indicates the mean squared displacement from the simulation of a freely diffusing bead is close to the theoretical displacement. The error never exceeds2.5% during the trials.

These two metrics validate the accuracy of the stochastic model.

Table 4.1: Simulated mean squared displacement comparison with theoretical values for freely diffusing beads

Simulation Time (s)	**Simulated displacement** (m)	**Theoretical displacement** (m)	**Magnitude Difference** (m)	**Percentage Error** (%)
10	8.77e-12	$8.58e-12$	1.94 e-13	2.25
20	1.74e-11	1.71e-11	2.88e-13	1.67
60	5.09e-11	5.15e-11	5.90e-13	1.14

4.2 Model Predictive Controller

The core controller we are utilizing is a stochastic model predictive controller (MPC). The MPC solves a receding horizon problem where at each step the system is simulated open loop but only the first input step is applied. The feedback received is then used to make the necessary corrections on the next step. The MPC uses the high fidelity dynamics model above to calculate the effects of the inputs on the future state of the system, thereby enabling it to plan a trajectory based on possible conditions that might arise. Since the dynamics model also takes into account the stochastic nature of the particles being controlled and the effect of multiple optical traps on a single particle the MPC is able to handle these uncertainties. The algorithm for the MPC is described below and visualized using a flowchart in Figure 4.3.

The first three lines of the algorithm ensure that a plan of input is created before hand until the objects are at their respective final destination. So while the objects are not yet at their final destination the input for that time step is applied and the feedback is used to check if the trapped objects are within the required margin of error to the estimated locations. If they are the next input can be applied. If they are not then the beams are re initialized to trap the objects again and the MPC computes a new input trajectory. This

Algorithm 1 MPC

Input:- y

Output:- $\mathbf{U}(t)$ until final time

1: Initialize trap locations as object centroid locations from images

2: Pick a destination for each object

3: System is simulated for a time horizon of t using Equation 4.4 where t is the time taken by the furthest object to reach its destination. The locations of the traps are calculated to optimize the following cost function (Equation 4.6) using a heuristic. The cost function reduces the error between the current positions and final destinations of all the objects at every time instance.

$$J = \sum_{i=0}^{t}((\mathbf{x}(i) - \mathbf{x}_d)^T(\mathbf{x}(i) - \mathbf{x}_d)) \tag{4.6}$$

The traps are limited to moving a maximum distance at each time step of the t-time horizon depending on the laser power and size of particle being moved

4: **while** objects are not at destinations **do**

5: **if** Read data and calculated estimate for step i do not match **then**

6: re initialize beams to current object locations

7: recalculate trajectory for $t - i$ time horizon

8: **else**

9: move traps to calculated locations from previous trajectory computation

10: **end if**

11: **end while**

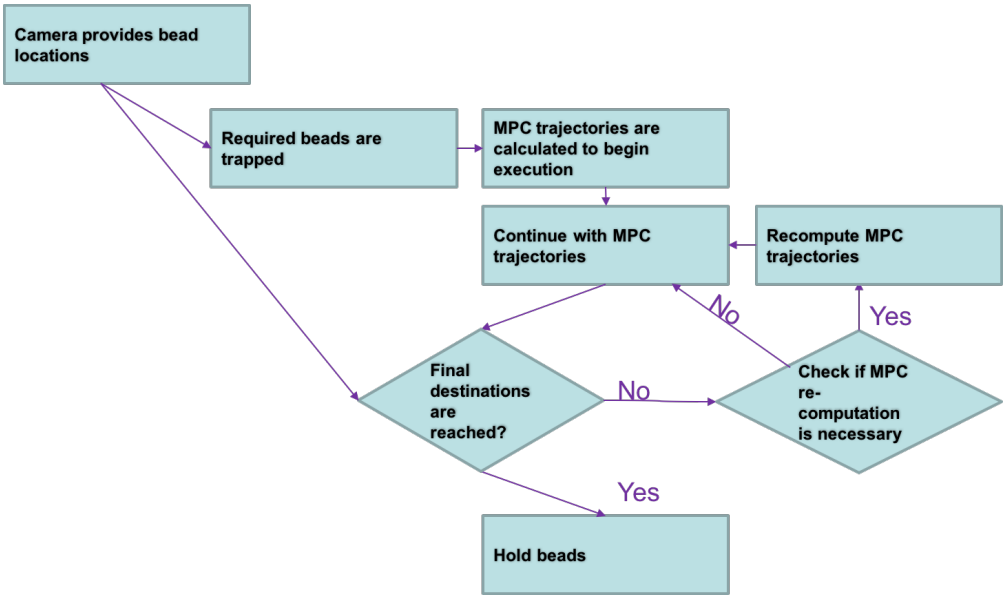

Figure 4.3: Flowchart for Algorithm 1

way computation occurs only when needed and not as at every step. This helps us keep pace with this highly stochastic system in real time.

4.3 Obstacle Avoidance

The MPC handles stochasticity and force coupling but does not actively avoid obstacles. To achieve obstacle free manipulation of the object we will layer a D* Lite algorithm over the MPC. D* Lite is a grid search based path planning algorithm [43]. It uses a heuristic cost and path cast to evaluate each path based on current state and future reward. It is similar to the Lifelong planning A* (LPA) [44] method in that it can adjust computed paths as new information is received. D* Lite has a few advantages over LPA. The heuristic calculated is fixed as it is calculated from a fixed point, the goal so lesser computations are necessary during path updates.It works with lesser space complexity as it is not necessary to keep track of the shortest path. So this algorithm provides a computationally effective method to deal with highly stochastic obstacles in the form of freely diffusing objects that are not actively

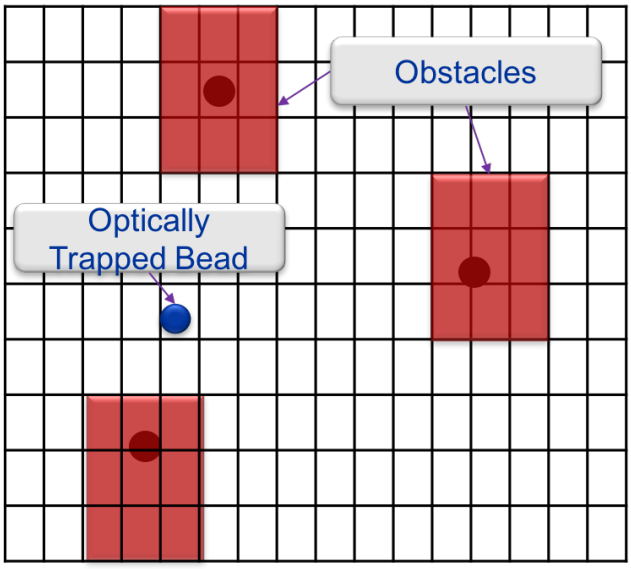

Figure 4.4: D* Lite Implementation

controlled.

4.3.1 D Lite Implementation*

The major issues that needs to be overcome is the response time between obstacle detection and the algorithm execution, accounting for the stochastic motion of the obstacles during the path computations. The reaction time needs to be fast as the obstacle can be trapped even if is not at the focus of the tweezing beam. Since the D* Lite needs to be run sequentially for all the objects and the computed path of the first needs to be valid after the last path is computed. Since improving computational efficiency can only help so much, we have modified a few aspects of the algorithm to help us achieve better performance in these aspects.

Discretization

The workspace is discretized into square grids of dimension equal to one diameter of the object being controlled. This ensures the grid world is in the same scale as the object of

interest. A visual representation of the discretized workspace can be seen in Figure 4.4.

Look Ahead

The controller looks ahead not just a single step but four steps to ensure that all of them are obstacle free. This way an obstacle is detected ahead of time and computation can occur before the object gets too close to the obstacle. This look ahead improves our response time and prevents unwanted trapping of objects. Since we repeatedly check the same point multiple times, we also effectively handle false negatives that may arise in the image processing or diffusion of particles from different planes than the one being imaged by the camera.

Effective area of obstacles

To make the lookahead effective and provide a margin of safety for the objects being controlled, we enlarge each obstacle with an effective area that is one diameter wide in all the directions. Thus, each obstacle is defined as a block of 3×3 to realize three benefits. First, it ensures that any path calculated is such that the obstacle is always outside the trapping area of the laser. Second, it ensures that any stochastic movement of the obstacle during computation is compensated such that the computed path is viable for a longer duration. Third, it limits path re-computations to only large movements of the obstacles, thereby reducing the computational workload and improving the response time. We choose an enlargement width of one diameter as anything smaller would not provide us with a sufficiently large safe region, and anything larger would create huge obstructed regions that are not only expensive to compute but would also prevent access to the goal nodes altogether. This is denoted by the red region around all obstacles in Figure 4.4.

Control Switching

The next issue is to decide on when and how to switch between the MPC and D* Lite. The MPC is initially used to calculate a globally optimum trajectory that tries to cover

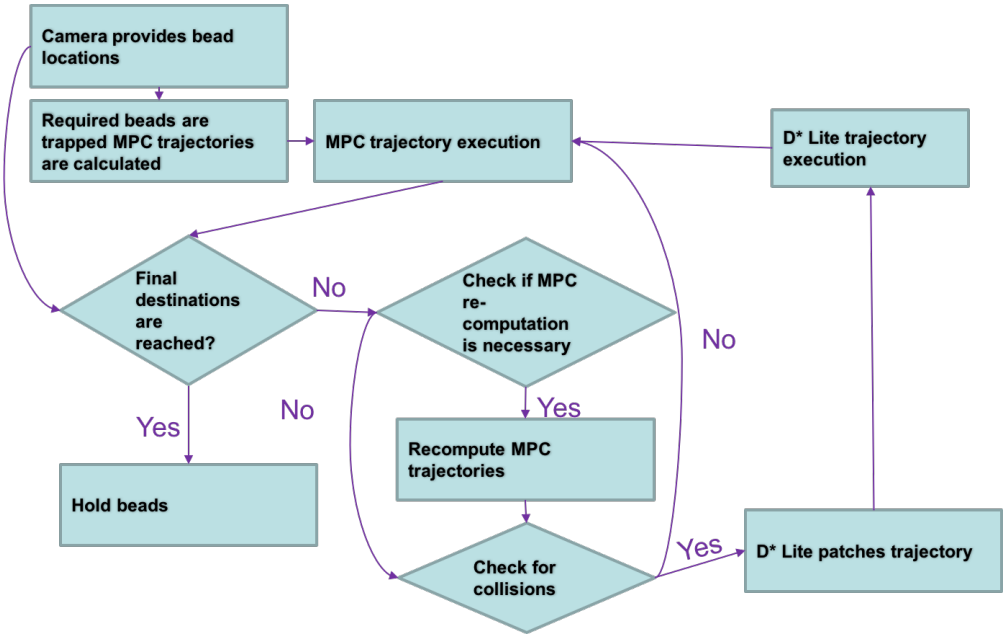

Figure 4.5: Flowchart for Algorithm 2

the maximum possible distance at every step. The D* Lite method is triggered only if this computed trajectory passes through one or more obstacles. It then stitches a collision free path between the current point and the next point on the MPC trajectory that is not obstructed. This stitching ensures that the path is globally optimum for the largest possible duration. Furthermore, is is computationally more efficient as the D* Lite method is not running continuously and it runs only for short path lengths. Computations occur only for the beads that are facing imminent collision and only for short path lengths thereby maintaining computational efficiency. The algorithm with the MPC and D* Lite together is described in Algorithm 2 and in the flowchart in Figure 4.5. A visual representation of how this switching works is provided by Figure 4.6.

We provide a ts pause at the end of executing any trajectory step as the optically trapped object requires a certain amount of time to physically move to the new location of the trap. If we do not have this delay, then the trapped object will be lost. The duration of the pause

Algorithm 2 MPC+OA

```
Fetch initial object locations using the Image Processing method
Trap the required number of objects.
Compute the trajectories for all the objects using the MPC method.
Set D* triggered for all objects to FALSE
while objects are not at their final destinations do
    Fetch workspace scene data using the Camera feedback.
    if all the trajectories are collision free then
        Execute the next steps in the MPC trajectories.
        if D* triggered is true and the goal of D* Lite trajectory is reached then
            Switch back to MPC trajectory.
        end if
        Pause for t seconds.
    else
        Check which object trajectories are obstructed.
        if D* Lite has not been triggered for the obstructed object then
            Set D* triggered as TRUE for the object under consideration.
            Update scene information using the Image Processing method.
            Locate closest free point on the remaining trajectory.
            Utilize the identified point as the goal and execute D* Lite.
            Switch from MPC trajectory to D* Lite trajectory.
        else
            if D* Lite goal is obstructed then
                Obtain new goal location and recalculate D* Lite trajectory.
            else
                Update scene and recalculate D* Lite trajectory.
            end if
        end if
    end if
end while
Maintain traps at their final locations.
```

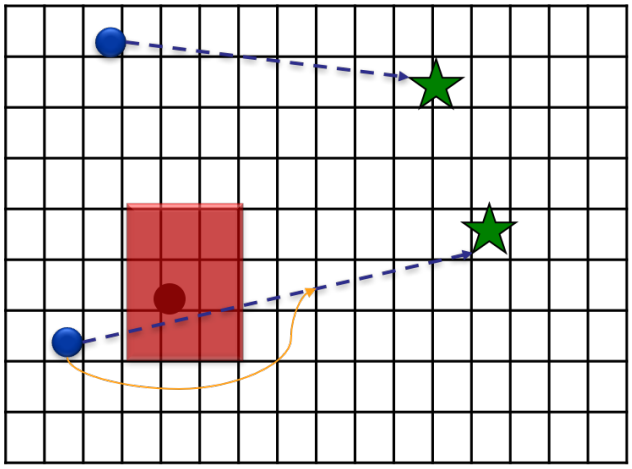

Figure 4.6: Control switching between MPC and D* Lite. MPC paths are indicated by the broken blue lines and the D* trajectory by the yellow line. The D* Lite creates a new path between two MPC path points and only for the bead that requires it.

depends on the size of the object, the relaxation time, and the distance covered by each step in the trajectory. A key assumption we make is that the final desired destination of the object is always free of obstacles. Any obstacle present in and around the final goal will be trapped. Hence, the goal location must either be vacant or needs to be cleared actively during execution by another subroutine.

Chapter 5

IMPLEMENTATION

Algorithm 1 and Algorithm 2 were tested in laboratory experiments with silica beads. The experiments were conducted with the CUBE (Meadowlark Optics, Inc., Frederick, CO, USA) HOT platform. The platform consists of an IPG Photonics YLR - Series laser (wavelength of 1070nm), a spatial light modulator, a dichroic beam-splitter and a camera. The objective used was an oil-immersion Olympus UApo N 340 lens with 40x magnification and 1.35 NA. The entire control algorithm was run on a Dell Precision M4600 laptop with Intel Core i5-2540M 2.60GHz processor and 4GB of RAM on a 64-bit Windows 7 Professional Operating System. Trap stiffnesses were computed using OTGO toolbox [14]. The control algorithm was written in C++ using Microsoft Visual Studio 2013 as the development platform.

The field of view of the workspace was 120 μm x 90 μm. The solution was prepared by mixing 100μl of the cloudy white 2.01 μm silica micro-sphere solution (Bangs Laboratories, Inc., Fishers, IN, USA) with 50ml water providing a dilution level of 500:1. A 1μl sample from the prepared diluted solution at room temperature was used for the experiments. A total laser power of 1.2 W was used.

5.1 Image Processing

The camera present in our Holographic Optical Tweezers (HOT) platform provides us with images of the workspace. From these images, we utilize our developed image processing method [12] to obtain the coordinates of all the beads in the workspace. From the raw image, the smudge marks are removed first using the the method described in [33]. On this smudge free image, we implement a Speeded Up Robust Features (SURF) algorithm to get the bead positions. SURF utilizes a Hessian matrix based detector to identify interest points

but saves time by using the same measure for both scale and location. The descriptors are extracted from a square region centered around the point of interest. The orientation of the region is determined by a circular region around the same point. The square is then split into sub regions from which feature information is extracted.

We are also able to detect partially visible beads in the workspace by using a combination of contrast limited adaptive histogram equalization (CLAHE) and Canny edge detection. To accomplish this, we first dilate the images then use the floodfill algorithm on the dilated images. Addition of the dilated images and the bitwise NOT operated floodfilled images removes any disturbances in contour detection of the beads. To overcome enlarging issues that occur during this process, both of the above mentioned images images are eroded first. Subtraction of the floodfilled version of the eroded image from the original eroded image provides us with the silhouettes of all partially visible beads in the borders of the workspace. The image processing method, thus, provides feedback to the model predictive controller and workspace state information to the control algorithm.

5.2 Experiments without Obstacle Avoidance

This section handles all results while running Algorithm 1 and so there is no active obstacle avoidance.

5.2.1 Four bead experiment

As shown in Figure 5.1, the beads are initially trapped and are moved towards their destination locations that forms a square grid. The Figures clearly illustrate the motion of the beads as time passes. At 12s into the experiment, two beads have already reached close to their destinations. After that period they hold that positions until the other beads are brought to their final positions.

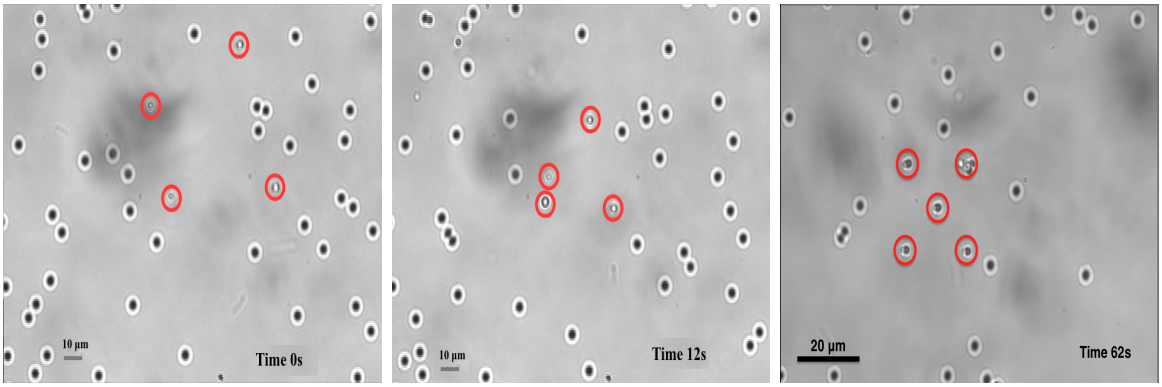

Figure 5.1: Experimental Results for the automated motion control of trapped beads to form a 2x2 grid pattern. The trapped beads are highlighted in red

5.2.2 Five bead experiment

Figure 5.2 show the results for a five bead experiment with only the MPC. As clearly seen in Figure 5.2b the controlled bead does not avoid the freely diffusing bead but traps it instead as seen in Figure 5.2c. The next few results will show that algorithm 2 is able to sense such obstacles and navigate around them. The beads reach their final destination and are held there henceforth.

5.3 Experiments with active Collision Avoidance

5.3.1 Four bead experiment

The trapped beads are shown using red circles.The obstacles detected by the image processing are bounded by yellow rectangles as seen in Figure 5.3b. Although the obstacles are really close to the initial position of a bead as seen in Figure 5.3b, D* Lite computation is fast enough for the bead to navigate past the obstacles as seen in Figure 5.3c, and reach its final destination.In Figure 5.3d we see that, since we do not clear the final destination beforehand, a bead present there gets trapped during the MPC trajectory execution.

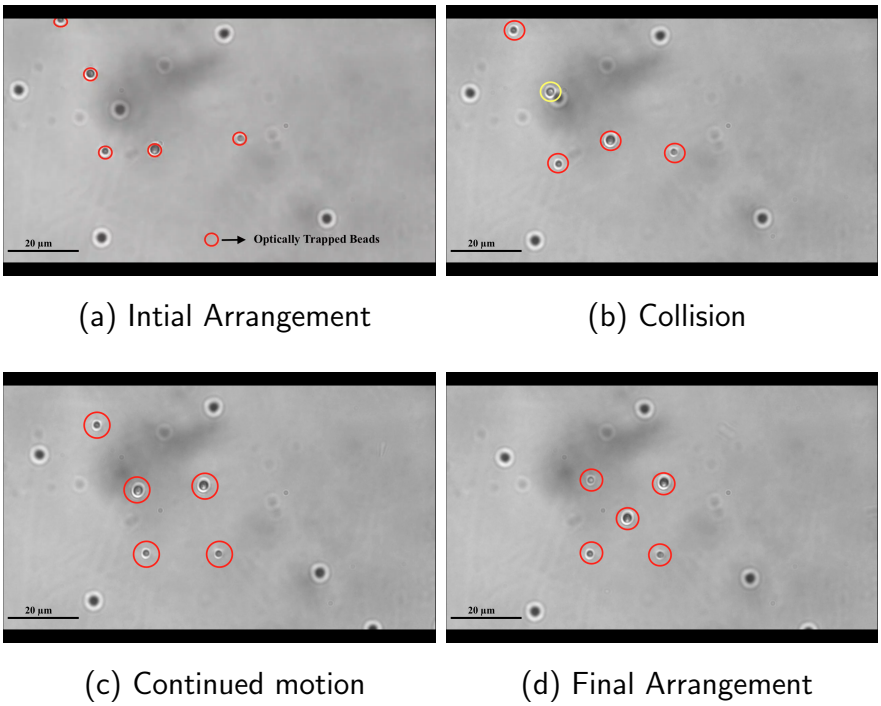

(a) Intial Arrangement (b) Collision

(c) Continued motion (d) Final Arrangement

Figure 5.2: Experimental results for automated transport of 5 beads All trapped beads are highlighted with a bounding circle. (a) Optically trapped beads are shown in their initial arrangements. (b) The bead marked in yellow collides with a freely diffusing bead (c) Execution continues with the calculated trajectory. (d) The beads are stably trapped at their goal locations

5.3.2 Five bead experiment

Again the trapped beads are shown using red circles.The obstacles detected by the image processing are bounded by yellow rectangles as seen in Figure 5.4b. The bead that executes D* Lite identifies a path in between the two detected obstacles. As the bead is performing obstacle avoidance, stochastic motions of the obstacles constrict the path that the bead is traversing in Figure 5.4c. Though the path is now constricted, due to the effective areas assigned to the obstacles initially, the path is just large enough for the bead to successfully

avoid collisions and reach the desired goal location.

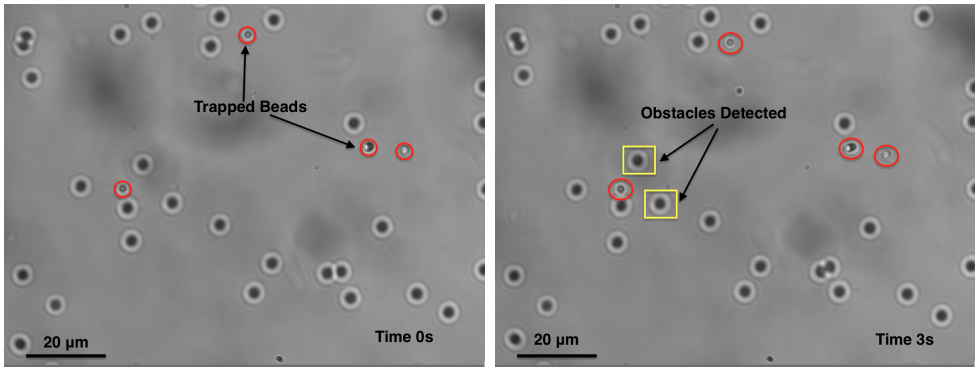

(a) Intial Arrangement (b) Obstacles Detected

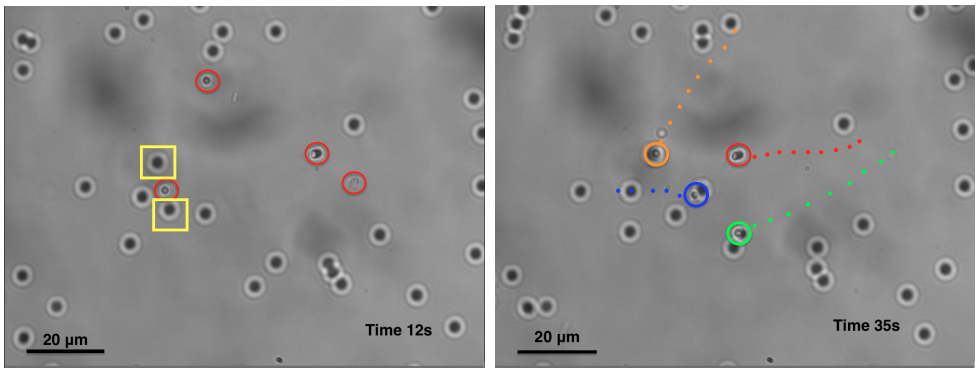

(c) Avoiding Obstacles (d) Final Arrangement

Figure 5.3: Experimental results for automated transport of 4 beads. (a) Optically trapped beads are shown in their initial arrangements. (b) The detected obstacles are shown using yellow rectangular boxes. The obstacles are detected along the path of just one bead. (c) The algorithm determines the shortest path while navigating past two obstacles. (d)The beads are stably trapped at their respective goal locations. The complete trajectories for the individual beads are shown using matching colored dots.

Table 5.1 shows the durations for which the MPC and D* Lite ran during the two experiments described above. Selectively running D* Lite ensures that the Optimal MPC trajectory runs for a large chunk of the total time and computations are minimized.

Table 5.1: Transport distance and execution times for the bead performing obstacle avoidance

No. of actively controlled beads	**Distance traversed**	**D* Lite (in s)**	**MPC (in s)**	**Final Position (in s)**
4	23 μm	12 s	12 s	11 s
5	45 μm	22 s	30 s	10 s

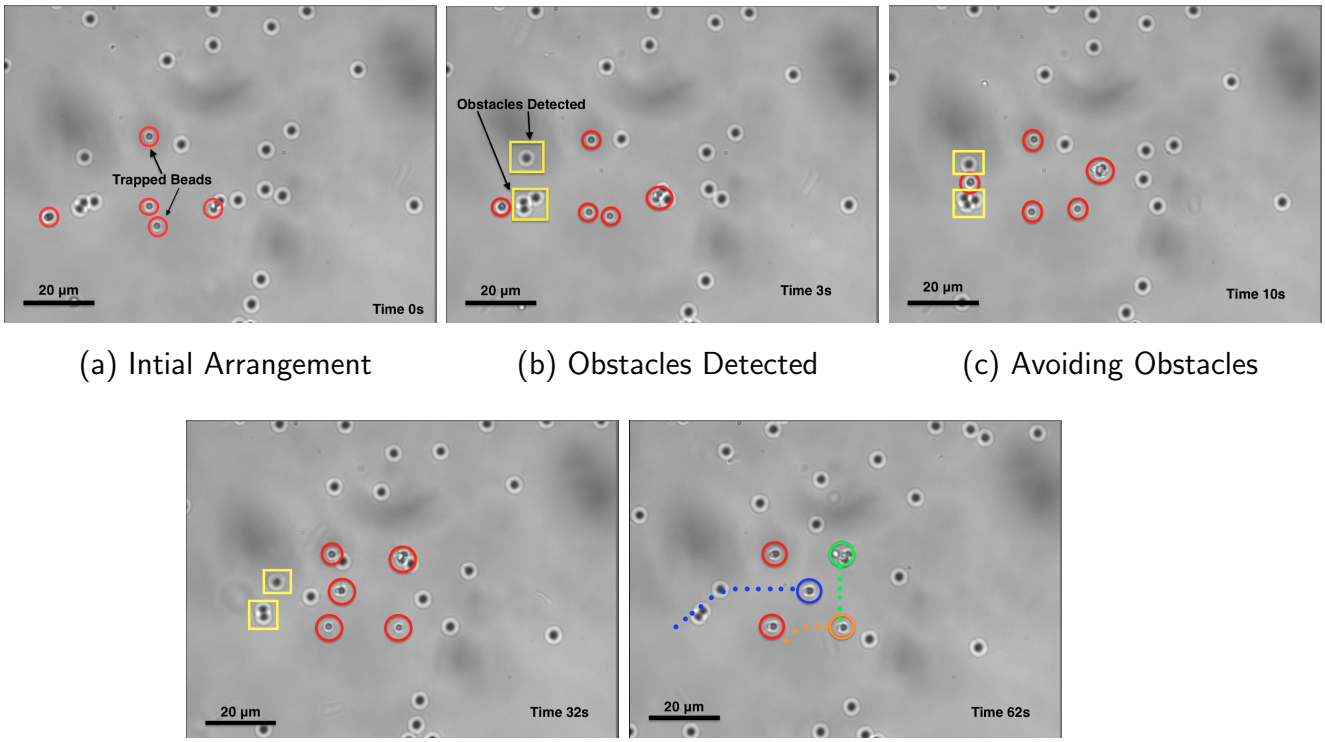

(a) Intial Arrangement (b) Obstacles Detected (c) Avoiding Obstacles

(d) Obstacles Avoided (e) Final Arrangement

Figure 5.4: Experimental results for automated transport of 5 beads. (a) Optically trapped beads are shown in their initial arrangements. (b) The detected obstacles are shown using yellow rectangular boxes. The obstacles are detected along the path of just one bead. (c) The algorithm determines the shortest path navigating in between the two obstacles. (d) The bead successfully navigates past the obstacle and continues towards its goal location. (e) The beads are stably trapped at their goal locations. The complete trajectories for the individual beads are shown using matching colored dots except for two beads that start very close to their final locations.

Chapter 6

CONCLUSION

This thesis presents a stochastic dynamics model for any given set of objects under the influence of multiple optical traps. It also details a real time Model Predictive Controller that has been experimentally proven to automatically control and move silica spheres to target locations and form useful arrangements. Further it also describes an algorithm to overlay add obstacle avoidance to the Model Predictive Controller. This algorithm was also experimentally verified to show that it is able to automatically control and move silica spheres to target locations and form useful arrangements while actively avoiding obstacles in the path of the controlled paths in real time. The method accounts for stochastic Brownian motions of the manipulated objects and the freely diffusing beads. The results are promising and affirm the usefulness of the method for manipulating more than two or three micro-scale objects in parallel while utilizing the mutiplexable capabilities of the Holographic Optical Tweezers system to the limit.

Chapter 7

ANTICIPATED IMPACT

There are two main fields where the system described in this thesis would find the most use.

1. Automated formation of micro-assemblies

   The HOT system with the algorithm described above could be used to yield precisely controlled granular micro-structures with enhanced properties. The algorithm should be able to handle the scale and complexity of the problem while providing precise manipulation.

2. Automated formation of multi-cellular patterns

   It should also provide a viable alternative for tissue engineering. The current preferred methods namely, micro molding and 3D bioprinting have issues creating complex structures like capillaries and veins. Using the system described above it should be possible to assemble these structures by moving individual cells into the formations necessary to replicate the tissue desired. It also provides a solution to precisely study cell communications.

Chapter 8

FUTURE WORK

This thesis proposes a methodology to leverage the multiplexing capabilities inherent in the Holographic Optical Tweezers. Before this can be applied to sectors mentioned above some more work needs to be done to refine and improve the performance of the algorithm. Factors like the maximum number of objects that can be manipulated concurrently, the required laser power, and the maximum transport speed need to be characterized using a larger set of experiments in workspaces of varying concentrations.

To prove robustness extensive experiments on solutions where the solution contains objects of different sizes and materials (e.g., polystyrene) will need to be conducted. The control framework can be adapted so as to manipulate motile microbes and other biological cells.

The computational efficiency of the algorithm can be vastly improved if the D* Lite computations are parallelized. Utilizing GPU programming to accomplish this would make it possible to manipulate more than ten beads concurrently.

BIBLIOGRAPHY

[1] Helene Andersson and Albert Van den Berg. Microfluidic devices for cellomics: a review. *Sensors and actuators B: Chemical*, 92(3):315–325, 2003.

[2] A Ashkin. Acceleration and trapping of particles by radiation pressure. *Phys Rev Lett*, 24:156–159, 1970.

[3] A. Ashkin. Forces of a single-beam gradient laser trap on a dielectric sphere in the ray optics regim. *Biophysical Journal*, 61, 1992.

[4] Ashis Gopal Banerjee, Arvind Balijepalli, Satyandra K. Gupta, and Thomas W. LeBrun. Generating simplified trapping probability models from simulation of optical tweezers system. *Journal of Computing and Information Science in Engineering*, 9, 2009.

[5] Ashis Gopal Banerjee, Sagar Chowdhury, Wolfgang Losert, and Satyandra K. Gupta. Survey on indirect optical manipulation of cells, nucleic acids, and motor proteins. *Journal of Biomedical Optic*, 05, 2011.

[6] Ashis Gopal Banerjee, Sagar Chowdhury, Wolfgang Losert, and Satyandra K. Gupta. Real-time path planning for coordinated transport of multiple particles using optical tweezers. *IEEE Transactions on automation science and engineering*, 9(4), 2012.

[7] Ashis Gopal Banerjee and Satyandra K. Gupta. Research in automated planning and control for micromanipulation. *IEEE Transactions on automation science and engineering*, 10(3), 2013.

[8] Ashis Gopal Banerjee, Wolfgang Losert, and Satyandra K. Gupta. A decoupled and prioritized stochastic dynamic programming approach for automated transport of multiple particles using optical tweezers. *Volume 6: ASME Power Transmission and Gearing Conference; 3rd International Conference on Micro- and Nanosystems; 11th International Conference on Advanced Vehicle and Tire Technologies*, 2009.

[9] Ashis Gopal Banerjee, Andrew Pomerance, Wolfgang Losert, and Satyandra K. Gupt. Developing a stochastic dynamic programming framework for optical tweezer-based automated particle transport operations. *IEEE Transactions on automation science and engineering*, 7(2), 2010.

[10] David J Beebe, Glennys A Mensing, and Glenn M Walker. Physics and applications of microfluidics in biology. *Annual review of biomedical engineering*, 4(1):261–286, 2002.

[11] Ali Asgar S Bhagat, Hansen Bow, Han Wei Hou, Swee Jin Tan, Jongyoon Han, and Chwee Teck Lim. Microfluidics for cell separation. *Medical and Biological Engineering and Computing*, 48(10):999–1014, 2010.

[12] M. Bollavaram, P. Sane, S. Chowdhury, S. K. Gupta, and A. G. Banerjee. Automated detection of live cells and microspheres in low contrast bright field microscopy. *Proceedings of International Conference on Manipulation, Automation and Robotics at Small Scales (MARSS)*, 2016.

[13] E. F. Camacho C. (Carlos) Bordons. *Model predictive control*. Springer, New York, 1962.

[14] Agnese Callegari, Mite Mijalkov, A. Burak Gkz, and Giovanni Volpe. computational toolbox for optical tweezers in geometrical optics. *J. Opt. Soc. Am. B*, 32:B11–B19, 2015.

[15] Mark Cannon and Basil Kouvaritakis. Optimizing prediction dynamics for robust mpc. *IEEE Transactions on Automatic Control*, 50(11):1892–1897, 2005.

[16] Stephen C. Chapin, Vincent Germain, and Eric R. Dufresne. Automated trapping, assembly, and sorting with holographic optical tweezers. *Optics express*, 14(26), 2006.

[17] C. C. Cheah, X. Li, X. Yan, and D. Sun. Simple pd control scheme for robotic manipulation of biological cell. *IEEE Transaction on automatic control*, 60(5), 2015.

[18] Chien Chern Cheah, Xiang Li, Xiao Yan, and Dong Sun. Observer-based optical manipulation of biological cells with robotic tweezers. *IEEE Transactions on Robotics*, 30(1):68–80, 2014.

[19] Haoyao Chen, Jian Chen, and Dong Sun. A novel allocation-based formation algorithm for swarm of micro-scaled particles. In *Robotics and Automation (ICRA), 2011 IEEE International Conference on*, pages 1664–1669. IEEE, 2011.

[20] Haoyao Chen and Dong Sun. Pairing and moving swarm of micro particles into array with a robot-tweezer manipulation system. In *Intelligent Robots and Systems (IROS), 2011 IEEE/RSJ International Conference on*, pages 451–456. IEEE, 2011.

[21] Haoyao Chen and Dong Sun. Automatic flocking manipulation of micro particles with robot-tweezers technologies. In *Robotics and Automation (ICRA), 2012 IEEE International Conference on*, pages 4588–4593. IEEE, 2012.

[22] Haoyao Chen and Dong Sun. Swarm-inspired transportation of biological cells using saturation-controlled optical tweezers. In *Robotics and Automation (ICRA), 2015 IEEE International Conference on*, pages 3531–3536. IEEE, 2015.

[23] Haoyao Chen, Can Wang, Xiaojian Li, and Dong Sun. Transportation of multiple biological cells through saturation-controlled optical tweezers in crowded microenvironments. *IEEE/ASME Transactions on Mechatronics*, 21(2):888–899, 2016.

[24] Sagar Chowdhury, Petr Svec, Chenlu Wang, Wolfgang Losert, and Satyandra K. Gupta. Gripper synthesis for indirect manipulation of cells using holographic optical tweezers. *IEEE International Conference on Robotics and Automation*, 2012.

[25] Sagar Chowdhury, Petr Svec, Chenlu Wang, Kevin T. Seale, John P. Wikswo, Wolfgang Losert, and Satyandra K. Gupta. Investigation of automated cell manipulation in optical tweezers-assisted microfluidic chamber using simulations. *Volume 7: 5th International Conference on Micro- and Nanosystems; 8th International Conference on Design and Design Education; 21st Reliability, Stress Analysis, and Failure Prevention Conference*, 2011.

[26] Sagar Chowdhury, Atul Thakur, Chenlu Wang, Petr Svec, Wolfgang Losert, and Satyandra K. Gupta. Automated indirect transport of biological cells with optical tweezers using planar gripper formations. *IIEEE International Conference on Automation Science and Engineering*, pages 267–272, 2012.

[27] Jennifer E Curtis, Brian A Koss, and David G Grier. Dynamic holographic optical tweezers. *Optics communications*, 207(1):169–175, 2002.

[28] CR Cutler and BL Ramaker. Aiche national meeting. *Houston, USA, WP5-B*, 1979.

[29] Edsger W Dijkstra. A note on two problems in connexion with graphs. *Numerische mathematik*, 1(1):269–271, 1959.

[30] František Duchoň, Andrej Babinec, Martin Kajan, Peter Beňo, Martin Florek, Tomáš Fico, and Ladislav Jurišica. Path planning with modified a star algorithm for a mobile robot. *Procedia Engineering*, 96:59–69, 2014.

[31] Dave Ferguson and Anthony Stentz. Field d*: An interpolation-based path planner and replanner. *Robotics research*, pages 239–253, 2007.

[32] Bjarne A Foss, Tor A Johansen, and Aage V Sørensen. Nonlinear predictive control using local modelsapplied to a batch fermentation process. *Control Engineering Practice*, 3(3):389–396, 1995.

[33] J. Gu, R. Ramamoorthi, P. Belhumeur, and S. Nayar. Removing image artifacts due to dirty camera lenses and thin occluders. *ACM Trans. Graphics*, 28(5), 2009.

[34] S. F. Gull. Developments in maximum-entropy data analysis. In J. Skilling, editor, *Maximum Entropy and Bayesian Methods*, pages 53–71. Kluwer Academic, Dordrecht, 1989.

[35] K. M. Hanson. Introduction to Bayesian image analysis. In M.H̃. Loew, editor, *Medical Imaging: Image Processing*, volume 1898 of *Proc. SPIE*, pages 716–731, 1993.

[36] Yasuhiro Harada and Toshimitsu Asakura. Radiation forces on a dielectric sphere in the rayleigh scattering regime. *Optics Communications*, 124:529–541, 1996.

[37] Peter E Hart, Nils J Nilsson, and Bertram Raphael. A formal basis for the heuristic determination of minimum cost paths. *IEEE transactions on Systems Science and Cybernetics*, 4(2):100–107, 1968.

[38] Silvia Hormeno and J Ricardo Arias-Gonzalez. Exploring mechanochemical processes in the cell with optical tweezers. *Biology of the Cell*, 98(12):679–695, 2006.

[39] Tao Ju, Shuang Liu, Jie Yang, and Dong Sun. Apply rrt-based path planning to robotic manipulation of biological cells with optical tweezer. In *Mechatronics and Automation (ICMA), 2011 International Conference on*, pages 221–226. IEEE, 2011.

[40] Tao Ju, Shuang Liu, Jie Yang, and Dong Sun. Path planning for 3d transportation of biological cells with optical tweezers. In *Automation and Logistics (ICAL), 2011 IEEE International Conference on*, pages 40–45. IEEE, 2011.

[41] Lydia E Kavraki, Petr Svestka, J-C Latombe, and Mark H Overmars. Probabilistic roadmaps for path planning in high-dimensional configuration spaces. *IEEE transactions on Robotics and Automation*, 12(4):566–580, 1996.

[42] Donald E. Knuth. *The TEX book*. Addison-Wesley, 1984.

[43] Sven Koenig and Maxim Likhachev. Dˆ* lite.

[44] Sven Koenig, Maxim Likhachev, and David Furcy. Lifelong planning a. *Artificial Intelligence*, 155(1-2):93–146, 2004.

[45] James J Kuffner and Steven M LaValle. Rrt-connect: An efficient approach to single-query path planning. In *Robotics and Automation, 2000. Proceedings. ICRA'00. IEEE International Conference on*, volume 2, pages 995–1001. IEEE, 2000.

[46] X. Li and C. C. Cheah. Dynamic region control for robot-assisted cell manipulation using optical tweezers. *2012 IEEE International Conference on Robotics and Automation*, 2012.

[47] Xiang Li and Chien Chern Cheah. Robotic cell manipulation using optical tweezers with unknown trapping stiffness and limited fov. *IEEE/ASME Transactions on Mechatronics IEEE/ASME Trans. Mechatron.*, 20(4):16241632, 2015.

[48] N. Malagnino, G. Pesce, A. Sasso, and E. Arimondo. Measurements of trapping efficiency and stiffness in optical tweezers. 214:15–24, 2002.

[49] David Q Mayne, James B Rawlings, Christopher V Rao, and Pierre OM Scokaert. Constrained model predictive control: Stability and optimality. *Automatica*, 36(6):789–814, 2000.

[50] Timo A. Nieminen, * Norman R. Heckenberg, and Halina Rubinsztein-Dunlop. Forces in optical tweezers with radially and azimuthally polarized trapping beams. *Optics letters*, 33(2), 2008.

[51] Timo A Nieminen, Vincent L Y Loke, Alexander B Stilgoe, Gregor Knoner, Agata M Branczyk, Norman R Heckenberg, and Halina Rubinsztein-Dunlo. Optical tweezers computational toolbox. *J. Opt. A: Pure Appl. Opt*, 9:468–471, 2007.

[52] Masahiro Ohshima, Hiromu Ohno, Iori Hashimoto, Mikiro Sasajima, Masayuki Maejima, Keiichi Tsuto, and Tadaharu Ogawa. Model predictive control with adaptive disturbance prediction and its application to fatty acid distillation column control. *Journal of Process Control*, 5(1):41–48, 1995.

[53] Frauke Oldewurtel, Alessandra Parisio, Colin N Jones, Dimitrios Gyalistras, Markus Gwerder, Vanessa Stauch, Beat Lehmann, and Manfred Morari. Use of model predictive control and weather forecasts for energy efficient building climate control. *Energy and Buildings*, 45:15–27, 2012.

[54] B Pluymers, JA Rossiter, JAK Suykens, and Bart De Moor. A simple algorithm for robust mpc. *IFAC Proceedings Volumes*, 38(1):257–262, 2005.

[55] Keshav Rajasekaran, Manasa Bollavaram, and Ashis G Banerjee. Toward automated formation of microsphere arrangements using multiplexed optical tweezers. In *Society of Photo-Optical Instrumentation Engineers (SPIE) Conference Series*, volume 9922, 2016.

[56] Giulio Ripaccioli, Daniele Bernardini, Stefano Di Cairano, Alberto Bemporad, and IV Kolmanovsky. A stochastic model predictive control approach for series hybrid electric vehicle power management. In *American Control Conference (ACC), 2010*, pages 5844–5849. IEEE, 2010.

[57] Robert M. Simmons, Jeffrey T. Finer, Steven Chu, and James A. Spudi. Quantitative measurements of force and displacement using an optical trap. *Biophysical Jour*, 70, 1996.

[58] N. R. Heckenberg T. A. Nieminen, H. Rubinsztein-Dunlop and A. I. Bishop. Numerical modelling of optical trapping. *Computer Physics Communications*, 142:468–471, 2001.

[59] Y. Tanaka, K. Hirano, H. Nagata, and M. Ishikawa. Real-time three-dimensional orientation control of non-spherical micro-objects using laser trapping. *Electron. Lett. Electronics Letters*, 43(7):412, 2007.

[60] Yoshio Tanaka, Hiroyuki Kawada, Ken Hirano, Mitsuru Ishikawa, and Hiroyuki Kitajima. Automated manipulation of non-spherical micro- objects using optical tweezers combined with image processing techniques. *Optics Express*, 16(19), 2008.

[61] Giorgio Volpe and Giovanni Volp. Simulation of a brownian particle in an optical trap. *Am. J. Phys*, 81(224), 2013.

[62] Xiaolin Wang, Shuxun Chen, Marco Kong, Zuankai Wang, Kevin D Costa, Ronald A Li, and Dong Sun. Enhanced cell sorting and manipulation with combined optical tweezer and microfluidic chip technologies. *Lab on a Chip*, 11(21):3656–3662, 2011.

[63] Mitchel Weissbluth. *Photon-atom interactions*. Academic Press, 2012.

[64] Xiao Yan, Chien Chern Cheah, Quang Minh Ta, and Quang-Cuong Pham. Stochastic dynamic trapping in robotic manipulation of micro-objects using optical tweezers. *IEEE Trans. Robot. IEEE Transactions on Robotics*, 32(3):499512, 2016.

[65] Hu Zhang and Kuo-Kang Liu. Optical tweezers for single cells. *Journal of The Royal Society Interface*, 5(24):671–690, 2008.

[66] Zhanying Zhang and Ziping Zhao. A multiple mobile robots path planning algorithm based on a-star and dijkstra algorithm. *International Journal of Smart Home*, 8(3):75–86, 2014.